EXHIBIT "C"

ELSEVIER

Journal of Membrane Science 208 (2002) 269–283

journal of MEMBRANE SCIENCE

www.elsevier.com/locate/memsci

Modeling of modified atmosphere packaging based on designs with a membrane and perforations

D.R. Paul [a,*], R. Clarke [b]

[a] *Department of Chemical Engineering, Texas Materials Institute, University of Texas, Austin, TX 78712, USA*
[b] *Landec Corporation, 3603 Haven Avenue, Menlo Park, CA 94025, USA*

Received 9 January 2002; received in revised form 8 May 2002; accepted 31 May 2002

Abstract

The freshness of fruits and vegetables can be prolonged by storage in an optimum atmosphere of oxygen and carbon dioxide that slows the respiratory process. The technology known as modified atmosphere packaging (MAP) seeks to create such an environment passively during shipping, storage, and marketing of produce. It is shown here that the combination of a high flux membrane (selective permeation of gases) patch with perforations (or holes that provide non-selective permeation of gases) in the package film offer a versatile route to create whatever oxygen and carbon dioxide environment may be needed for a given product. Detailed mathematical models are developed here for describing and designing such systems. Particular attention is devoted to the steady-state analysis where produce respiration is balanced by transport into and out of the package. The perforations serve the dual function of allowing convective flow of gases to prevent package volume shrinkage and non-selective permeation of gases to adjust the ratio of CO_2/O_2 transport. Detailed predictive models for both functions are developed.
© 2002 Elsevier Science B.V. All rights reserved.

Keywords: Permeation; Membranes; Modified atmosphere packaging; Convection; Modeling

1. Introduction

Prolonging the freshness or shelf life of fruits and vegetables after harvest is important for ensuring a safe and nutritional diet at an affordable cost. Low temperature storage is a major means of preserving freshness of post-harvest produce. However, storage under reduced O_2 and elevated CO_2 partial pressures can provide an additional means of reducing metabolic activity and increasing shelf life [1–25]. Membrane technology can be used to regulate the gaseous atmosphere surrounding produce during various phases of its distribution and is currently practiced in some instances. Controlled atmosphere storage refers to exposing produce continuously to some desired, constant gas composition, typically during bulk storage or shipping. Conventional gas separation membrane modules can be used to create this gaseous atmosphere at a fixed storage site or on-board the transportation system used for shipping. On the other hand, modified atmosphere packaging (MAP) is a passive means of creating an altered gas composition around the produce in packages during shipping and marketing, typically in small plastic packages [1–25]. The objective of this paper is to show how high flux membrane "labels" combined with perforations in the package can be used to create an optimum gaseous environment within a package for prolonging the

* Corresponding author. Tel.: +1-512-471-5392; fax: +1-512-471-542.
E-mail address: drp@che.utexas.edu (D.R. Paul).

0376-7388/02/$ – see front matter © 2002 Elsevier Science B.V. All rights reserved.
PII: S0376-7388(02)00303-4

freshness of fruits and vegetables. The literature describes various aspects of modeling the gas exchange process for MAP applications [12–25]; however, the development presented here is more complete and unique in several regards.

2. Post-harvest plant physiology

In contrast to some other perishable foods (e.g. meats), fresh fruits and vegetables continue to respire after harvesting [1–10]. Respiration involves a complex set of biochemical processes of which part is the oxidative breakdown of starch, sugars and organic acids into CO_2 and H_2O plus heat and metabolic energy. The respiration rate and metabolic pathway may change naturally as the produce goes through the internal processes of ripening, maturity and senescence or be changed artificially by altering the external environment of storage, i.e. temperature and surrounding gas composition. The objective of controlled or modified atmosphere storage is to lower the rate of respiration through atmosphere management (in addition to temperature control) to reduce the rate of substrate depletion, O_2 consumption, CO_2 production, and the associated heat release [1,4,6]. Senescence begins as the stored starch and sugar is consumed; the rate of substrate consumption is simply determined by the rate of respiration. Consequently, shelf life is inversely related to the respiration rate [1,4,6].

A great deal of experimental evidence has shown that the respiration rate depends on the concentration of O_2 and CO_2 in which the produce is stored after harvesting. Various types of mathematical models for describing these relationships have been developed. Some are simply empirical fits of experimental data [13,14] while others are based on the principles of enzyme kinetics [8,9]. The latter have the form of the Michaelis–Menten kinetic equation with an added term to account for the inhibition due to CO_2 [8]. The suggested form for the rate of O_2 uptake is as follows:

$$r_{O_2} = \frac{WR_m p_{O_2}}{k_m + [1 + (p_{CO_2}/K_i)]p_{O_2}} \quad (1)$$

where p_{O_2} and p_{CO_2} are the partial pressures of O_2 and CO_2, W the mass of the produce, and R_m, k_m, and K_i are the temperature dependent parameters specific to a particular type of produce. An analogous equation can be written for the rate of CO_2 production, r_{CO_2}. The ratio of CO_2 produced to O_2 consumed is known as the respiratory quotient, i.e.

$$RQ = \frac{r_{CO_2}}{r_{O_2}} \quad (2)$$

This ratio can range from about 0.7 to 1.4 depending on the substrate and its metabolic state [1–6]; an RQ value of 1.2 is typical [13–16].

While reducing the oxygen partial pressure can increase shelf life, it is essential that the oxygen level not be reduced to the point that anaerobic respiration occurs. Anaerobiosis results in formation of ethanol, acetaldehyde, and organic acids (fermentation) which may cause undesirable odors and flavors. Of greater concern is that formation of anaerobic pathogens, such as Clostridium botulinum, which may not cause any organoleptic degradation and, thus, the food may appear unspoiled yet cause food poisoning [1,2,4,6,11]. Consequently, oxygen levels must be maintained at high enough levels to prevent this scenario.

Carbon dioxide is more than a by-product of respiration. It is widely recognized as an inhibitor of the growth of certain types of bacteria and fungi [1,2,6]. The mechanism of CO_2 inhibition, which affects both the lag phase and the growth rate, is not fully understood but is related to its dissolution in the fluid phases and perhaps consequent chemical activity. Also, as suggested by Eq. (1), elevated CO_2 levels inhibit O_2 consumption. In any case, shelf life is further prolonged by storing fresh produce in finite CO_2 concentrations [1,2,6].

Based on the earlier discussion, it should be clear that for each type of produce there is an optimum range of O_2 and CO_2 concentrations that will lead to increased shelf life. There is a great deal of literature about the recommended ranges [4,7,22]. A convenient source of up-to-date information of this type is provided on a web site from the University of California at Davis, see http://postharvest.ucdavis.edu. Fig. 1 illustrates the recommended ranges for a number of fruits and vegetables selected to show the diversity of environments that are needed.

The purpose of this paper is to show how membrane technology can be used to achieve these gaseous environments in packages during isothermal storage. It is beyond the scope of this paper to discuss the

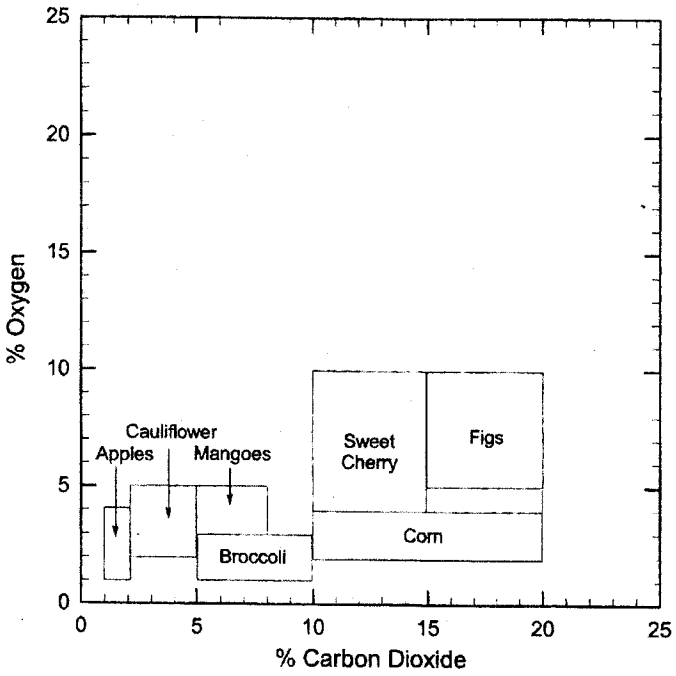

Fig. 1. The recommended ranges of oxygen and carbon dioxide concentrations that will prolong the shelf life of various fruits and vegetables. The data were taken primarily from the web site of the University of California at Davis (http://postharvest.ucdavis.edu).

detailed issues of the biological processes that occur during storage in these environments. We assume that the metabolic pathway is aerobic and do not consider the effects of other important environmental gases such as ethylene or water.

3. Semi-permeable packages

Fig. 2 schematically shows respiring produce stored in a package comprised of a plastic film. The simplest concept is to let the plastic film serve as the regulator of O_2 flow into the package and the flow of CO_2 out. However, in most cases, it is difficult to develop a plastic film that is permeable enough or thin enough to provide the needed O_2 and CO_2 transmission rates while meeting the other requirements of mechanical properties, appearance, and cost. Another approach is to incorporate non-selective holes or perforations in the bag [23,24] which has been commercially practiced for some time. A more recent approach has been to add a high flux membrane in the form of a patch or a label [26,27] which may or may not be selective. Correctly designed, the membrane can comprise a small fraction of the package area. High flux membranes of this kind can be of the asymmetric or composite types similar in construction to those employed for gas separations [28,29]. Such membranes consist of a porous substructure (for mechanical support and integrity onto which an ultra-thin, nearly defect-free, polymer skin resides (for permeation selectivity and rate control). The purpose of this paper is to model the performance of packages containing respiring produce that have both a permselective membrane and perforations. It will be shown that this combination offers a powerful way to control the composition of the O_2 and CO_2 in the package.

In this analysis, we will be concerned with the transmission of only three gases, O_2, CO_2 and N_2, in order to capture the main issues. For more sophisticated considerations, the transport of water vapor, ethylene, or other gases could be incorporated by a

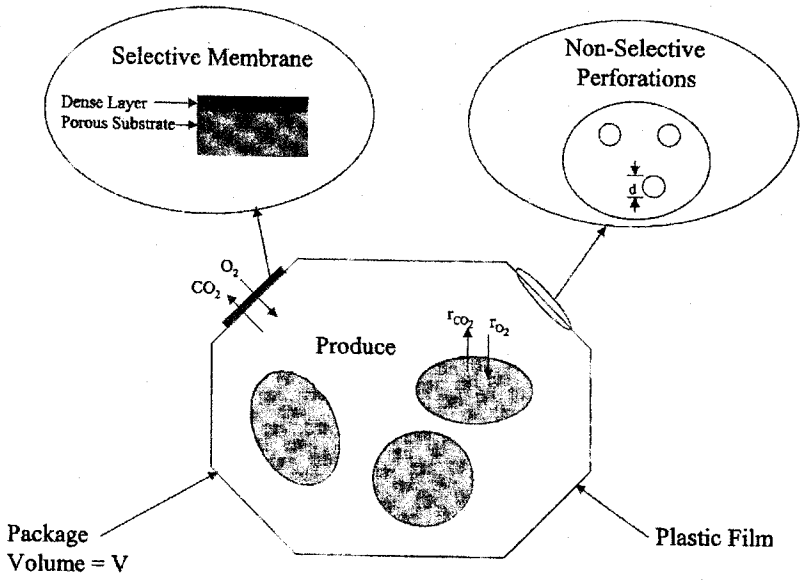

Fig. 2. Schematic illustration of produce in a plastic package outfitted with a selective membrane patch and non-selective perforations or holes.

simple extension of the model. For any gas i, its rate of permeation into the package can be represented by the following pseudo-steady-state relation:

$$\text{permeation rate of } i = K_i[(p_i)_o - (p_i)_i] \quad (3)$$

where $(p_i)_o$ is the partial pressure of i outside the package (atmosphere) and $(p_i)_i$ the partial pressure of i inside the package which in general varies with time. The parameter K_i describes the parallel permeation of gas i through the package film itself (area, A_p; thickness, ℓ_p; permeability, P_{pi}) and the membrane (area, A_m; effective thickness of dense skin, ℓ_m; permeability, P_{mi}) is given by

$$K_i = \left[\frac{A_m P_{mi}}{\ell_m} + \frac{A_p P_{pi}}{\ell_p}\right] \quad (4)$$

Generally, the contribution of the membrane (m) term will be much greater than that of the package film (p). In practice, the membrane can be designed to give the needed value of K_i at a given temperature by the choice of the polymer (P_{mi}) and by appropriately adjusting thickness and area (ℓ_m and A_m).

An important design parameter is the permselectivity of the package for the gases O_2, CO_2 and N_2. For systems where a dense polymer membrane or film controls the transport of gases into and out of the package, the permselectivity at a given temperature is fixed by the polymer choice and cannot be adjusted by either effective thickness or permeation area. A review of the available literature reveals that for the polymers that might reasonably be considered for such applications, the permselectivities lie approximately in the following ranges:

$$2 < (K_{CO_2}/K_{O_2}) < 10$$

$$2 < (K_{O_2}/K_{N_2}) < 6$$

Of these, the CO_2/O_2 ratio is the most important, and often one would like to have greater flexibility in specifying this ratio than practical membrane materials permit for two reasons that can be made quantitatively clear by model equations to be developed later. First, since K_{CO_2}/K_{O_2} generally will be much larger than the respiratory quotient, RQ, there will be more CO_2 leaving the package than O_2 entering. Nitrogen cannot make up the volumetric difference, so the package free volume tends to shrink during storage; sometimes to an unacceptable extent. This volume shrinkage can

be eliminated by introducing a very small hole that allows a convective influx of air to balance the total pressure inside the bag with the air outside. This, of course, alters the composition of the gas in the package relative to what it would have been in the absence of the hole. Second, one often needs a lower CO_2/O_2 permeation ratio than available polymer choices permit in order to achieve the CO_2/O_2 compositions for optimal extension of shelf life, see Fig. 1. This can be solved by making the area of the perforations/holes large enough to provide non-selective permeation in parallel with the membrane; this amounts to reducing the net CO_2/O_2 permeation ratio. Thus, to design effective packages, it is necessary to know how to model the combined convection/permeation functions of holes. This is developed in the next section.

4. Gas transmission through holes

We assume that the package film illustrated in Fig. 2 has n circular holes (or perforations) of diameter d; thus, the area of each hole $A_h = \pi d^2/4$. A very slight difference in the total pressures inside and outside the package will cause a net convective flow Q (taken as positive when the flow is into the package) such that the package free volume remains essentially constant. The size of the hole (or area) needed for pressure equalization can be shown to be quite small. The purpose here is to understand how to model the permeation response of gas i as a result of a difference in the partial pressure of i inside and outside (or a difference in mole fraction, x_i) where the total pressures on the two sides are essentially the same. First, a general model for the simultaneous convection and diffusion of gas i is developed followed by a more specific geometric model for the diffusion/permeation part. Finally, an experimental validation of the permeation model is given.

4.1. General model for simultaneous diffusion and convection through holes

The gas transmission through perforations in the package film involves both convection (flow required to equalize pressure) and diffusion (owing to mole fraction gradients) contributions. It is a good approximation to treat the gas phase as a pseudo-binary mixture comprised of component i ($i = O_2$, N_2, and CO_2 in turn) and all the rest of the gas mixture m; a more rigorous treatment as a ternary mixture in terms of say the Stefan–Maxwell equations [23,24,30] is an unjustified complication since the various binary diffusion coefficients are so similar, see Table 1. Fick's first law for the flux of gas i, N_i, can be written in the following general form [30] within the approximation suggested

Table 1
Binary gas diffusion coefficients at 25 °C[a]

Gas pair	D_{ij} (cm²/s)
Oxygen/nitrogen	0.21
Oxygen/carbon dioxide	0.15
Nitrogen/carbon dioxide	0.15

[a] Calculated from the kinetic theory of gases [30].

$$N_i = x_i \sum_{j=1} N_j - cD_{im} \nabla x_i \tag{5}$$

where x_i is the mole fraction of gas i, c the total molar gas concentration ($c = p/RT$, where p is the total gas pressure, R the gas constant, T the temperature), and D_{im} the diffusion coefficient for gas i in the gas mixture. Fig. 3 shows an expanded view of the geometry of a cylindrical hole in the film which will be useful in later discussions. The convective flux of gas through this hole (along the axial direction z) is given by

$$\widehat{Q} = \sum_{j=1} N_{jz} = \frac{Q}{nA_h} \tag{6}$$

Thus, within the hole, Eq. (5) can be written in its unidimensional form as

$$N_{iz} = x_i \widehat{Q} - cD_{im} \frac{dx_i}{dz} \tag{7}$$

The multi-axial components of the resistance to mass transport at the entrance and exit to the hole can be treated by assigning an effective length, ℓ_{eff}, of the hole that is greater than its geometric length ℓ. With these simplifications, Eq. (7) can be integrated with the appropriate boundary conditions to obtain the following steady-state result

$$\frac{N_{iz} - (x_i)_i \widehat{Q}}{N_{iz} - (x_i)_o \widehat{Q}} = \exp\left(\frac{\widehat{Q}\ell_{eff}}{cD_{im}}\right) = \xi \tag{8}$$

where $(x_i)_o$ and $(x_i)_i$ are the mole fractions of gas i in the atmosphere outside the package and in the gas

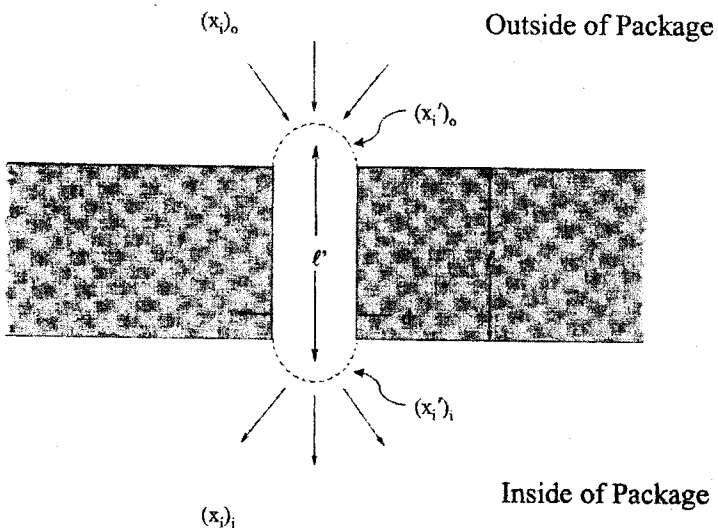

Fig. 3. Schematic of the geometry of a cylindrical hole in the package film used in the development of a model for gas "permeation" through such a hole.

mixture within the package, respectively. For small enough values of $\widehat{Q}\ell_{\text{eff}}/cD_{\text{im}}$, the exponential term can be expanded into a series which can be truncated after the second term, i.e.

$$\xi \approx 1 + \frac{\widehat{Q}\ell_{\text{eff}}}{cD_{\text{im}}} \tag{9}$$

Combining Eq. (8) with the approximation of Eq. (9) gives

$$N_{iz} = \frac{cD_{\text{im}}}{\ell_{\text{eff}}}[(x_i)_o - (x_i)_i] + (x_i)_o\widehat{Q} \tag{10}$$

which applies for the case of $\widehat{Q} > 0$, i.e. the convective flow is into the package. This equation shows that the convective and diffusive (or permeation) functions of the hole are additive within the approximations made; the assumption implicit in Eq. (9) turns out to be well justified. The total permeation of gas i through all the holes is given by

$$\frac{nA_h cD_{\text{im}}}{\ell_{\text{eff}}}[(x_i)_o - (x_i)_i] = \frac{nA_h D_{\text{im}}}{\ell_{\text{eff}}RT}[(p_i)_o - (p_i)_i] \tag{11}$$

Since the D_{ij} are so similar for the various binary pairs of the O_2, N_2, CO_2 mixture (see Table 1), it is justified to assume that $D_{\text{im}} = D_{jm} = D_{ij}$ [30] and ignore any selectivity of diffusive transport through the holes. Thus, it is convenient to define the following term:

$$H = \frac{nA_h D_{\text{im}}}{\ell_{\text{eff}}RT} \tag{12}$$

to describe the diffusive transport of each gas through the perforations. In the following section, a model is developed for calculation of ℓ_{eff} in terms of geometrical parameters.

4.2. Hole permeation model

The diffusion of gas from the outside atmosphere, through the hole, and then to the inside of the package (or vice versa) can be treated by breaking the problem into the series resistances of these three zones which in Fig. 3 are divided by dotted lines defined by hemispheres of diameter equal to that of the hole, d. Uniaxial diffusion is assumed in the region within the hole to the boundaries of the two hemispheres; the equivalent cylindrical length of this zone ℓ' is estimated from the ratio of its volume to its cross-sectional area, i.e.

$$\ell' = \frac{(\pi/4)d^2\ell + (\pi/6)d^3}{(\pi/4)d^2} = \ell + \frac{2}{3}d \tag{13}$$

Thus, the total molar diffusive transport of i through this region M_i is given by

$$M_i = A_h N_{iz} = \frac{\pi d^2 c D_{im}}{4\ell'}[(x'_i)_o - (x'_i)_i] \quad (14)$$

where the x'_i are the mole fractions of i on the surfaces of the hemisphere (dotted lines in Fig. 3) on the outside and inside of the package. The mass transfer in the regions external to the two hemispheres is modeled in terms of radial diffusion from infinity to the surface of each hemisphere. The mass transfer coefficient k_{x_i} for this case is given by

$$k_{x_i} = \frac{2cD_{im}}{d} \quad (15)$$

that is, the Nusselt number is 2 [30].

For the region entering the hole:

$$M_i = \left(\frac{\pi d^2}{2}\right) k_{x_i}[(x_i)_o - (x'_i)_o] \quad (16)$$

and for the region exiting the hole:

$$M_i = \left(\frac{\pi d^2}{2}\right) k_{x_i}[(x'_i)_i - (x_i)_i] \quad (17)$$

where $\pi d^2/2$ is the area of the hemisphere. Combining Eqs. (13)–(17) gives

$$M_i = A_h N_{iz} = \left(\frac{\pi d^2}{4}\right) \frac{cD_{im}[(x_i)_o - (x_i)_i]}{[\ell + (7/6)d]} \quad (18)$$

In other words, the ℓ_{eff} in Eqs. (10) and (11) is given by

$$\ell_{eff} = \ell + \frac{7}{6}d \quad (19)$$

and H defined by Eq. (12) is

$$H = \frac{nA_h D_{im}}{[\ell + (7/6)d]RT} \quad (20)$$

Section 4.3 provides experimental validation of Eq. (20).

4.3. Experimental validation of hole permeation model

The simple apparatus illustrated in Fig. 4 was used to demonstrate experimentally that Eq. (20) adequately describes the "permeation" properties of circular holes. The device consists of a metal cylinder (internal volume, $V = 134.5\,cm^3$) to which an oxygen analyzer (model C-44611 R22 from Teledyne Instruments Inc.) was attached to one end. An opening on the other end accommodated interchangeable plates

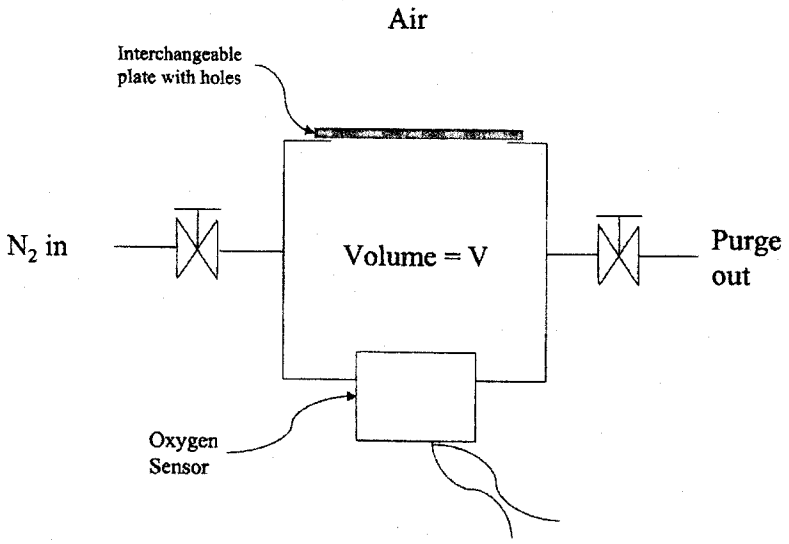

Fig. 4. Diagram of experimental apparatus used to measure permeation through holes.

into which holes (from 1 to 5) were drilled; the plates varied in thickness from 0.00284 to 0.102 cm while the hole diameters ranged from 0.0762 to 0.127 cm. The cylinder was purged with pure nitrogen through the lines shown in Fig. 4 while the holes were blanked off by masking tape. At time zero, the valves were closed and the tape was removed. Thus, oxygen from the surrounding air permeated through the holes into the cylinder. The oxygen content in the cylinder was measured as a function of time by the sensor.

The rate of oxygen accumulation in the cylinder is given by

$$\frac{dn_{O_2}}{dt} = \frac{V}{RT}\frac{d(p_{O_2})_i}{dt} = H[(p_{O_2})_o - (p_{O_2})_i] \quad (21)$$

where n_{O_2} is the moles of oxygen that have permeated in time t, $(p_{O_2})_i$ the partial pressure of oxygen in the cylinder at time t, and $(p_{O_2})_o$ the partial pressure of oxygen in the air surrounding the cylinder. Dividing Eq. (21) by the total pressure in the cylinder which is equal to the total pressure of the surrounding air allows this result to be expressed in terms of oxygen mole fractions

$$\frac{V}{RT}\frac{d(x_{O_2})_i}{dt} = H[(x_{O_2})_o - (x_{O_2})_i] \quad (22)$$

Eq. (22) can be integrated for calculation of H from measured x_{O_2} versus time data. However, the following differential form proved more useful

$$H = \frac{V}{RT}\frac{1}{(x_{O_2})_o}\left(\frac{d(x_{O_2})_i}{dt}\right)_{t=0} \quad (23)$$

where the derivative is the initial slope of the oxygen signal versus time.

Various combinations of hole dimensions and number were used for measurement of H at 25 °C. The experimental results are plotted in Fig. 5 (solid points) as a function of $n(\pi d^2/4)/[\ell + (7/6)d]$ as suggested by Eq. (22). The solid line in Fig. 5 was calculated from Eq. (20) using the value of the oxygen/nitrogen diffusion coefficient listed in Table 1. The good agreement between the data and the model indicates that Eq. (20)

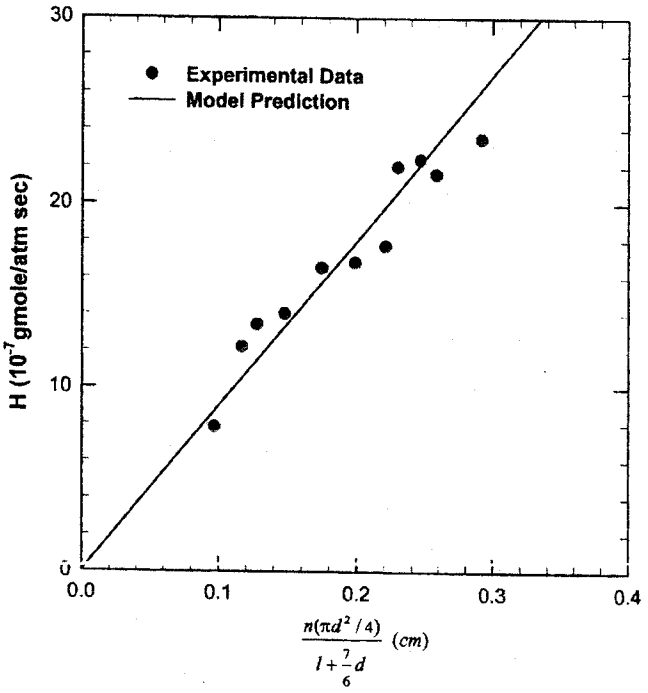

Fig. 5. Experimental measurements (points) and theoretical predictions (lines) of the mass transfer through holes by permeation, i.e. no total pressure differences between inside and outside. The data are plotted in the manner suggested by Eq. (20).

can be used with confidence. For well-defined perforations in the package film, the film thickness ℓ_p can be used for ℓ in this calculation. A value of the binary gas diffusion coefficient of the order of 0.18 cm^2/s (see Table 1) would seem appropriate.

5. Time dependent MAP models

The composition of the gas within the package illustrated in Fig. 2 can be modeled by a series of balance equations that consider the accumulation, generation, and transport of each of the gas species. In these equations, we will replace the partial pressure of species i with its mole fraction x_i; the two are related by

$$p_i = p_t x_i \tag{24}$$

To further simplify the notation, we will equate $(x_{O_2})_0 = 0.21$, $(x_{N_2})_0 = 0.79$, and $(x_{CO_2})_0 = 0$ to give the composition of the air outside the package and use x_i without a subscript to denote the composition inside the package (which we assume is spatially uniform throughout the package). The ideal gas law gives the moles of gas i in the package

$$n_i = \frac{x_i p_t V}{RT} \tag{25}$$

For constant temperature, the time rate of change of n_i is given by

$$\frac{dn_i}{dt} = \frac{p_t}{RT}\left[V\frac{dx_i}{dt} + x_i\frac{dV}{dt}\right] \tag{26}$$

provided we assume the total pressure is constant which for flexible packages is essentially the external atmospheric pressure. As mentioned earlier, we assume the gas in the package is comprised of O_2, N_2 and CO_2.

In most cases of interest, the convective flow is pure air into the package, i.e. $Q > 0$, and the three balance equations are as follows:

$$\frac{p_t}{RT}\left[V\frac{dx_{O_2}}{dt} + x_{O_2}\frac{dV}{dt}\right] = -r_{O_2} + (K_{O_2} + H)p_t[0.21 - x_{O_2}] + 0.21Q \tag{27}$$

$$\frac{p_t}{RT}\left[V\frac{dx_{CO_2}}{dt} + x_{CO_2}\frac{dV}{dt}\right] = r_{CO_2} + (K_{CO_2} + H)p_t[0 - x_{CO_2}] \tag{28}$$

$$\frac{p_t}{RT}\left[V\frac{dx_{N_2}}{dt} + x_{N_2}\frac{dV}{dt}\right] = (K_{N_2} + H)p_t[0.79 - x_{N_2}] + 0.79Q \tag{29}$$

For the more unusual case where the convective flow is reversed, i.e. $Q < 0$, and the gas within the package flows out, then the balance equations become

$$\frac{p_t}{RT}\left[V\frac{dx_{O_2}}{dt} + x_{O_2}\frac{dV}{dt}\right] = -r_{O_2} + (K_{O_2} + H)p_t[0.21 - x_{O_2}] + x_{O_2}Q \tag{30}$$

$$\frac{p_t}{RT}\left[V\frac{dx_{CO_2}}{dt} + x_{CO_2}\frac{dV}{dt}\right] = r_{CO_2} + (K_{CO_2} + H)p_t[0 - x_{CO_2}] + x_{CO_2}Q \tag{31}$$

$$\frac{p_t}{RT}\left[V\frac{dx_{N_2}}{dt} + x_{N_2}\frac{dV}{dt}\right] = (K_{N_2} + H)p_t[0.79 - x_{N_2}] + x_{N_2}Q \tag{32}$$

The sum of either set of three balance equations, i.e. Eqs. (27)–(29) or (30)–(32), leads to the following:

$$\frac{p_t}{RT}\frac{dV}{dt} = r_{CO_2} - r_{O_2} + \sum_i K_i \Delta x_i + Q \tag{33}$$

since,

$$x_{O_2} + x_{CO_2} + x_{N_2} = 1 \tag{34}$$

The term Δx_i is the mole fraction of i in the atmosphere minus that in the package. Note that all terms in H drop out in the summation. There are two well-defined limiting cases. In one, there is no convective flow ($Q = 0$) which would be the case if there were no holes; hence, H in Eqs. (27)–(32) would be zero. In this situation, Eq. (33) provides a means of calculating the rate of change of the package free volume (for most cases of interest, it shrinks) from knowledge of the composition of the gas in the package. In the other limiting case, there is convective flow such that the package volume remains constant ($dV/dt = 0$). For this situation, Eq. (33) provides one means of computing Q from knowledge of the composition of the gas in the package.

The composition of the gas inside the package can be computed numerically by solving the appropriate

set of differential equations, i.e. Eq. (33) (with either $Q = 0$ or $dV/dt = 0$) plus Eqs. (27)–(29) or (30)–(32). This is beyond the scope of the current paper. Instead, the focus of the remainder of this paper will be to explore the steady-state composition of gas in the package that can be reached after some initial transient period. The length of time to steady-state can be shortened by keeping the package free volume small or eliminated entirely by purging the package, when the produce is added, with a gas mixture of the same composition that is attained during steady-state.

The assumption of spatial uniformity of gas composition within the package made earlier can be justified by a simple calculation. We take the package dimension to be on the order of 10 cm and the gaseous diffusion coefficient to be 0.18 cm^2/s. Thus, the time scale for composition gradient relaxation, i.e. $(10\,cm)^2/0.18\,cm^2/s$, is of the order of 10 min; whereas, the storage times of interest are many days.

6. Steady-state MAP model

We are interested here in exploring the composition of the gas inside the package after a steady-state has been reached for the case where the package free volume, V, does not change. For most of the attainable x_{O_2} versus x_{CO_2} (see Fig. 1) region of interest, the convective flow term Q will be positive. Thus, from Eqs. (27)–(29), we can write the following for the steady-state regime:

$$-r_{O_2}(x_{O_2}, x_{CO_2}) + (K_{O_2} + H)p_t[0.21 - x_{O_2}] + 0.21Q = 0 \tag{35}$$

$$r_{CO_2}(x_{O_2}, x_{CO_2}) + (K_{CO_2} + H)p_t[0 - x_{CO_2}] = 0 \tag{36}$$

$$(K_{N_2} + H)p_t[0.79 - x_{N_2}] + 0.79Q = 0 \tag{37}$$

The respiration terms are written in a notation to remind us that these rates do depend on gas composition in the package; however, in the final steady-state equation that results from combining Eqs. (34)–(36), these terms appear only as the ratio r_{CO_2}/r_{O_2}; a great deal of experimental evidence suggests that the respiratory quotient is relatively independent of gas composition over most of the region of aerobic respiration [13,14,16,19].

Eqs. (36) and (37) can be rewritten as

$$x_{CO_2} = \frac{r_{CO_2}}{(K_{CO_2} + H)p_t} \tag{38}$$

$$Q = -\frac{p_t}{0.79}(K_{N_2} + H)(0.79 - x_{N_2}) \tag{39}$$

Thus, we see that these equations are valid only when $x_{N_2} > 0.79$ or $(x_{O_2} + x_{CO_2}) < 0.21$ since this is the region where $Q > 0$. By substituting Eqs. (2), (34), (38) and (39) into Eq. (35), we find that the possible steady-state values of x_{O_2} and x_{CO_2} lie on a straight line, i.e.

$$x_{O_2} = 0.21 - Cx_{CO_2} \tag{40}$$

where

$$C = \frac{0.21 - x_{O_2}}{x_{CO_2}} = \frac{(1/RQ)[(K_{CO_2} + H)/(K_{O_2} + H)] + 0.266[(K_{N_2} + H)/(K_{O_2} + H)]}{1 + 0.266[(K_{N_2} + H)/(K_{O_2} + H)]} \tag{41}$$

In the regions where $Q > 0$, a family of such lines of different slopes C can be designed for a given RQ by adjusting H and the K_i. Of all the steady-state atmospheres that are possible along this line, the one attained for a given situation is that which also satisfies Eq. (38) simultaneously.

For design purposes, it is useful to define a new parameter β as follows:

$$\beta = \frac{H}{K_{O_2}} \tag{42}$$

The straight line representing the possible steady-states given by Eq. (40), see Fig. 6, has intercepts of $x_{O_2} = 0.21$ when the carbon dioxide fraction is zero and $(x_{CO_2})_0$ when the oxygen mole fraction is zero. The latter mathematical quantity can be written as

$$(x_{CO_2})_0 = \frac{0.21}{C} = 0.21\frac{1 + 1.266\beta + 0.266(K_{N_2}/K_{O_2})}{[(K_{CO_2}/K_{O_2}) + \beta]/RQ + 0.266(K_{N_2}/K_{O_2} + \beta)} \tag{43}$$

by making use of Eqs. (35) and (42). Fig. 7 shows how $(x_{CO_2})_0$ varies with K_{CO_2}/K_{O_2} and RQ for the special case where H or β is zero (no permeation through

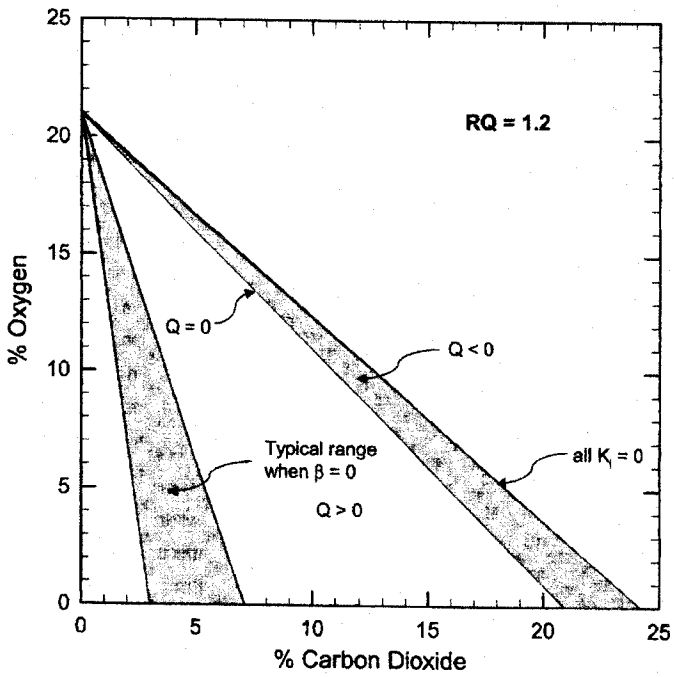

Fig. 6. Steady-state relationships between oxygen and carbon dioxide contents for MAP systems of various designs. When convective flow through the perforations is into the package (i.e. the region where $Q > 0$), the x_{O_2} vs. x_{CO_2} relationship is linear. The shaded region to the left shows the family of lines that can be attained for most polymer membrane materials in the absence of non-selective permeation through holes. The shaded region on the right indicates the small region where the convective flow is out of the package ($Q < 0$) where non-linear equations describe the relationship between steady-state O_2 and CO_2 levels in the package.

holes) for a value of $K_{O_2}/K_{N_2} = 3$. As it turns out, the value of $(x_{CO_2})_0$ is not very sensitive to the K_{O_2}/K_{N_2} selectivity of the membrane, at least within the range of 2–6 which is typical for common polymers. As seen, $(x_{CO_2})_0$ decreases, or the slope C increases, as K_{CO_2}/K_{O_2} increases and as RQ decreases. However, for typical values of the various parameters, $(x_{CO_2})_0$ is restricted to a fairly narrow range of values in the range of about 3–7%.

As may be seen by Eq. (39), the convective term vanishes, i.e. $Q = 0$, when $x_{N_2} = 0.79$. In this case, $C = 1$ and $(x_{CO_2})_0 = 0.21$; thus, the steady-states lie on the line

$$x_{O_2} = 0.21 - x_{CO_2} \tag{44}$$

This will occur when

$$\frac{K_{CO_2} + H}{K_{O_2} + H} = \frac{K_{CO_2}/K_{O_2} + \beta}{1 + \beta} = \mathrm{RQ} \tag{45}$$

The convective flow term is negative, i.e. $Q < 0$, when $x_{N_2} < 0.79$ which can occur when the parameter β is large enough and RQ is greater than one. At steady-state, Eqs. (30)–(32), which apply when $Q < 0$, cannot be reduced to a simple linear relation between x_{O_2} and x_{CO_2} because of the nature of the convection terms. Since the resulting equations are quite complex, no attempt is made to show them here. Nevertheless, it is useful to analyze the limiting case where there is no semi-permeable membrane, i.e. all $K_i = 0$; however, there is permeation through perforations, i.e. $H > 0$. The steady-state form of Eq. (32) gives

$$Q = -\frac{H(0.79 - x_{N_2})}{x_{N_2}} \tag{46}$$

The sum of the balance Eqs. (30)–(32) leads to

$$Q = -r_{O_2}(\mathrm{RQ} - 1) \tag{47}$$

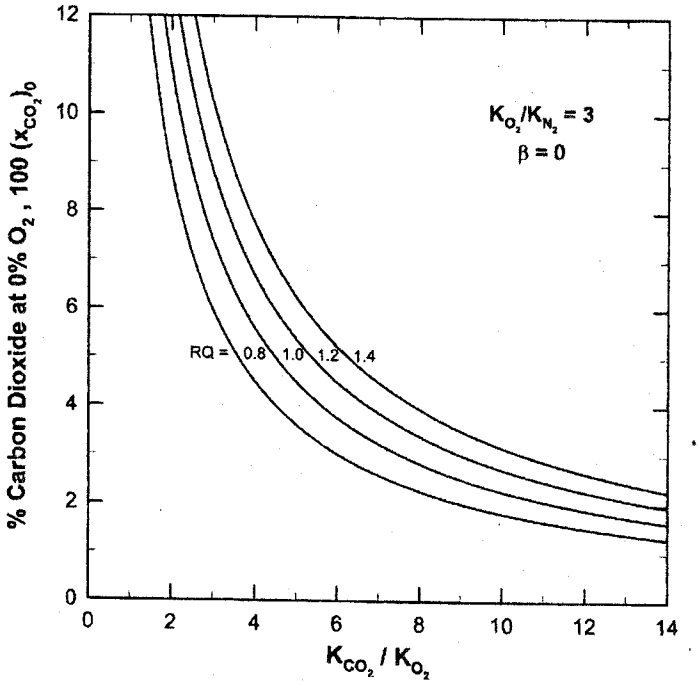

Fig. 7. In terms of the mathematical analysis, the carbon dioxide level in the package reaches a maximum value of $(x_{CO_2})_0$ when the oxygen content goes to zero. This plot shows the model calculations of $(x_{CO_2})_0$ as a function of K_{CO_2}/K_{O_2} and RQ when $K_{O_2}/K_{N_2} = 3$. It is important to note that $(x_{CO_2})_0$ is purely a mathematical concept since when the oxygen mole fraction is zero, anaerobic conditions are established and some of the basic assumptions of the analysis are no longer valid.

The relationships between the possible steady-state values of x_{O_2} and x_{CO_2} are once again linear and given by

$$x_{O_2} = 0.21 - \left[\frac{0.21\text{RQ} + 0.79}{\text{RQ}}\right] x_{CO_2} \tag{48}$$

The particular value of x_{CO_2} for a given design is

$$x_{CO_2} = \frac{r_{CO_2}}{H + (\text{RQ} - 1)r_{O_2}} \tag{49}$$

The intercept on the x_{CO_2} axis when $x_{O_2} = 0$ is given by

$$(x_{CO_2})_0 = \frac{0.21\text{RQ}}{0.21\text{RQ} + 0.79} \tag{50}$$

For the typical value of RQ = 1.2, $(x_{CO_2})_0 = 0.242$.

It is now possible to see the versatility that combining permselective membranes with perforations offers for MAP design. Fig. 8 shows $(x_{CO_2})_0$ as a function of the fraction of the O_2 permeation that occurs through holes, i.e. $\beta/(1+\beta)$, when the membrane selectivities have typical values of $K_{CO_2}/K_{O_2} = 4$ and $K_{O_2}/K_{N_2} = 3$ and the produce has typical values of RQ. When RQ = 1.2, the intercept on the carbon dioxide axis, see Fig. 6, can be as low as 6.6% CO_2 or as high as 24.2%. Thus, by comparison with Fig. 1, we can see that optimal atmospheres can be achieved at steady-state for many fruits and vegetables by adjusting the available design parameters.

It is useful to see the range of applicability of the models for the different Q regimes in the context of Fig. 6 at steady-state. All of the space within the triangle defined by the line $x_{O_2} + x_{CO_2} = 0.21$ is described by the simple model based on $Q > 0$. The slope of the linear lines within this region become steeper as the package selectivity of CO_2 to O_2 permeation becomes greater; this occurs as β decreases or K_{CO_2}/K_{O_2} increases. The completely non-selective package follows the outermost line (where all $K_i = 0$). This is the

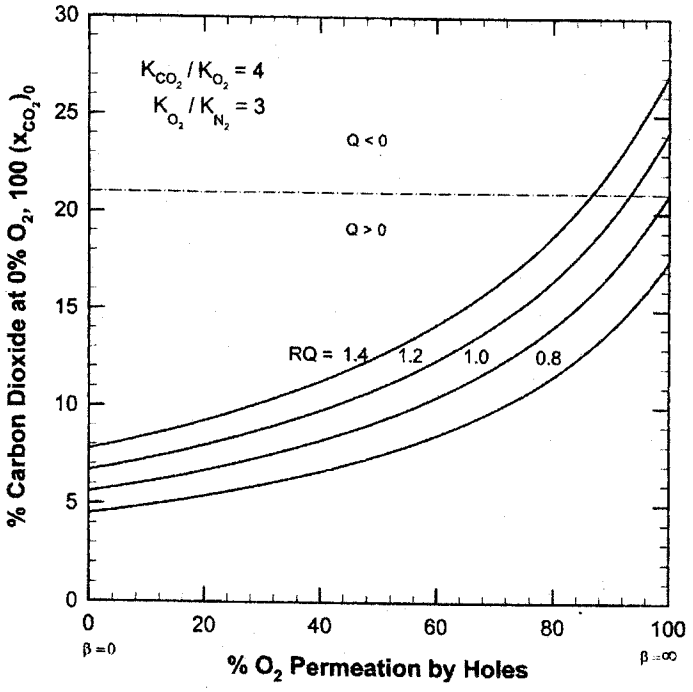

Fig. 8. Model predictions of $(x_{CO_2})_0$ for $K_{CO_2}/K_{O_2} = 4$ and $K_{O_2}/K_{N_2} = 3$ as the fraction of the total permeation through holes is varied. Over most of this region, the model for $Q > 0$ applies. The limits at $\beta = 0$ for $RQ > 1$ were calculated from the model for $Q < 0$.

line that would be followed by a package made from perforated film and no permselective membrane. For RQ = 1.2, the intercept of this line occurs at 24.2% CO_2. It is only the small shaded region between this outer line and the $Q = 0$ line where one must use the more complex equations that apply when $Q < 0$.

7. Some design considerations

The tendency for the package volume to shrink during storage of produce is inherent when gas exchange is entirely through a semi-permeable membrane made from currently known polymers. As we saw earlier, this problem can be conveniently eliminated by tiny holes that allow pressure equalization at constant volume by convective flow of gas. However, when the number or size of the holes is large enough, they also provide a useful way to alter the selectivity of gas exchange between the air and the package. The choice of a membrane material (and, hence, its permselectivity ratios K_i/K_j) determines the maximum slope or the intercept $(x_{CO_2})_0$ of steady-state plots of x_{O_2} versus x_{CO_2}, see Fig. 6. Addition of perforations offers a means to reduce this slope or increase $(x_{CO_2})_0$.

As seen by the calculations shown in Fig. 7, typical choices for polymeric materials used to fabricate the membrane patch lead to a relatively narrow range of carbon dioxide contents in the package at the limit of 0% oxygen, $(x_{CO_2})_0$, of the order of 3–7%. Thus, the steady-state relationships that are possible when $\beta = 0$ lie within the shaded triangle shown on the left in Fig. 6. On the other hand, simply using a perforated package leads to very high values of $(x_{CO_2})_0$; see line for $K_i = 0$ in Fig. 6 which applies when RQ = 1.2.

If Fig. 6 is overlaid onto Fig. 1, it is clear that the attainable regions when $\beta = 0$ or when all $K_i = 0$ exclude the possibility of providing the steady-state atmosphere inside packages that would be optimum for prolonging the shelf life of many types of fruits

and vegetables. The problem is that polymeric membranes are too selective in permeation of CO_2 relative to O_2 and perforations (holes) are not selective enough. However, by combining membrane and hole permeation in parallel, the attainable region of x_{O_2} versus x_{CO_2} can be expanded to include all the space between the two extremes illustrated in Fig. 6. This is illustrated by the calculations shown in Fig. 8. By appropriate selection of the membrane material and the relative extent of permeation through holes, packages can be designed having a x_{O_2} versus x_{CO_2} relation appropriate for most types of produce, see Fig. 1.

Another key issue is the absolute permeances of the package, i.e. $K_i + H$, relative to the absolute respiration rate. Largely, this is governed by the mass of produce relative to the membrane/hole areas for a given type of produce and membrane as shown by the following analysis. For simplicity, we take

$$K_{O_2} \approx A_m \left(\frac{P_{mO_2}}{\ell_m} \right) \tag{51}$$

$$r_{O_2} = Wf(x_{O_2}, x_{CO_2}) \tag{52}$$

We can rewrite Eq. (38) as

$$x_{CO_2} = \frac{r_{O_2} RQ}{K_{O_2}[(K_{CO_2}/K_{O_2}) + \beta] p_t} = \frac{Wf(x_{O_2}, x_{CO_2}) RQ}{A_m (P_{mO_2}/\ell_m)[(K_{CO_2}/K_{O_2}) + \beta] p_t} \tag{53}$$

and Eqs. (40) and (43) as

$$x_{O_2} = 0.21 \left[1 - \frac{x_{CO_2}}{(x_{CO_2})_0} \right] = 0.21 \left[1 - \left(\frac{W}{A_m} \right) \times \frac{f(x_{O_2}, x_{CO_2}) RQ}{(P_{mO_2}/\ell_m)(x_{CO_2})_0 [(K_{CO_2}/K_{O_2}) + \beta] p_t} \right] \tag{54}$$

For a given x_{O_2} versus x_{CO_2} line in Fig. 6, the values of RQ, $(x_{CO_2})_0$, K_{CO_2}/K_{O_2}, and β are all fixed. Thus, we see that the oxygen content in the package can be adjusted to the desired range by appropriately selecting the ratio of the mass of produce relative to the membrane area. Of course, the magnitude of membrane area needed for a given mass of produce depends on the permeance of the membrane, i.e. P_{O_2}/ℓ_m.

8. Summary and conclusions

An extensive literature and body of practical experience show that freshness of post-harvest fruits and vegetables can be significantly extended by storing them, while shipping or marketing, in an optimal atmosphere of oxygen and carbon dioxide that depends on the nature of the produce. It is shown here that a wide range of gas atmospheres can be created using a semi-permeable membrane patch in conjunction with perforations that provide non-selective permeation of gases between the air outside the package and the gas mixture inside the package. A model has been presented that considers the steady-state situation when the gas consumption/evolution by the respiring produce is exactly balanced with the permeation and convective transport of gas between the two environments. A model has been developed and experimentally validated for the "permeation" response of the perforations or holes. The overall model accounts for the simultaneous convective transport through the holes that is useful to control the package free volume. It is shown that almost all of the optimum atmospheres needed for maintaining freshness of a wide range of produce (see Fig. 1) can be created by modified atmosphere packaging based on appropriately designed systems that use combinations of a membrane and perforations as may be seen by overlaying Fig. 6 on Fig. 1.

The analysis given here considered the simple case where the package and its contents are stored at a fixed temperature. In practice, it is essential to consider the variations in temperature that may occur, especially during shipping, because both respiration and permeation depend on temperature, generally in very different ways. Approaches to deal with these issues will be the subject of future work.

Acknowledgements

This research was funded in part by National Science Foundation grant number CTS-0086961 administered by the Division of Chemical and Transport Systems-Separation and Purification Processes Program. The authors wish to thank Sharon Koshy for help with the experimental portions of this paper.

References

[1] D. Zagory, A.A. Kader, Modified atmosphere packaging of fresh produce, Food Technol. 42 (1988) 70.

[2] T.S. Lioutas, Challenges of controlled and modified atmosphere packaging: a food company's perspective, Food Technol. 42 (1988) 78.

[3] B. Ooraikul, M.E. Stiles (Eds.), Modified Atmosphere Packaging Of Food, Ellis Horwood, Chichester, 1991.

[4] R.T. Parry (Ed.), Principles and Applications of Modified Atmosphere Packaging of Food, Blackie, Glasgow, 1993.

[5] M.L. Rooney (Ed.), Active Food Packaging, Blackie, Glasgow, 1995.

[6] I.J. Church, A.L. Parsons, Modified atmosphere packaging technology: a review, J. Sci. Food Agric. 67 (1995) 143.

[7] L. Lee, J. Arul, R. Lencki, F. Castaigne, A review on modified atmosphere packaging and preservation of fresh fruits and vegetables: physiological basis and practical aspects (Part I), Packag. Technol. Sci. 8 (1995) 315;
L. Lee, J. Arul, R. Lencki, F. Castaigne, A review on modified atmosphere packaging and preservation of fresh fruits and vegetables: physiological basis and practical aspects (Part II), Packag. Technol. Sci. 9 (1996) 1.

[8] D.S. Lee, P.E. Haggar, J. Lee, K.L. Yam, Model for fresh produce respiration in modified atmospheres based on principles of enzyme kinetics, J. Food Sci. 56 (1991) 1581.

[9] Y. Makino, K. Iwasaki, T. Hirata, Application of transition state theory in model development for temperature dependence of fresh produce, J. Agric. Eng. Res. 67 (1997) 47.

[10] Y. Kubo, A. Inaba, R. Nakamura, Extinction point and critical oxygen concentration in various fruits and vegetables, J. Jpn. Soc. Hortic. Sci. 65 (1996) 397.

[11] B. Hintlian, J.H. Hotchkiss, The safety of modified atmosphere packaging: a review, Food Technol. 40 (1986) 70.

[12] A.C. Cameron, W. Boylan-Pett, J. Lee, Design of modified atmosphere packaging systems: modeling oxygen concentrations within sealed packages of tomato fruits, J. Food Sci. 54 (1989) 1413.

[13] R.M. Beaudry, A.C. Cameron, A. Shirazi, D.L. Dostal-Lange, Modified-atmosphere packaging of blueberry fruit: effect of temperature on package O_2 and CO_2, J. Am. Soc. Hortic. Sci. 117 (1992) 436.

[14] D.W. Joles, A.C. Cameron, A. Shirazi, P.D. Petracek, R.M. Beaudry, Modified-atmosphere packaging of "heritage" red raspberry fruit: respiratory response to reduced oxygen, enhanced carbon dioxide, and temperature, J. Am. Soc. Hortic. Sci. 119 (1994) 540.

[15] A.C. Cameron, R.M. Beaudry, N.H. Banks, M.V. Yelanich, Modified-atmosphere packaging of blueberry fruit: modeling respiration and package oxygen partial pressures a function of temperature, J. Am. Soc. Hortic. Sci. 119 (1994) 534.

[16] A.C. Cameron, P.C. Talasila, D.W. Joles, Predicting film permeability needs for modified-atmosphere packaging of lightly processed fruits and vegetables, Hortic. Sci. 30 (1995) 25.

[17] P.C. Talasila, A.C. Cameron, Free-volume changes in flexible, hermetic packages containing respiring produce, J. Food Sci. 62 (1997) 659.

[18] P.C. Talasila, A.C. Cameron, Prediction equations for gases in flexible modified-atmosphere packages of respiring produce are different than those for rigid packages, J. Food Sci. 62 (1997) 926.

[19] A.B. Smyth, J. Song, A.C. Cameron, Modified atmosphere packaged cut iceberg lettuce: effect of temperature and O_2 partial pressure on respiration and quality, J. Agric. Food Chem. 46 (1998) 4556.

[20] A. Exama, J. Arul, R.W. Lencki, L.Z. Lee, C. Toupin, Suitability of plastic films for modified atmosphere packaging of fruit and vegetables, J. Food Sci. 58 (1993) 1365.

[21] I. Merts, D.J. Cleland, N.H. Banks, A.C. Cleland, Mathematical model of a modified atmosphere packaging system for horticultural produce, Sci. Technol. Froid. 3 (1993) 443.

[22] L.Z. Lee, J. Arul, R. Lencki, F. Castaigne, Methodology for determining the appropriate selectivity of mass transfer devices for modified atmosphere packaging of fresh produce, Packag. Technol. Sci. 9 (1996) 55.

[23] D.S. Lee, P. Renault, Using pinholes as tools to attain optimum modified atmospheres in packages of fresh produce, Packag. Technol. Sci. 11 (1998) 119.

[24] P. Renault, M. Souty, Y. Chambroy, Gas exchange in modified atmosphere packaging. Part 1: a new theoretical approach for micro-perforated packs, Int. J. Food Sci. Technol. 29 (1994) 365.

[25] Y. Song, D.S. Lee, K.L. Yam, Predicting relative humidity in modified atmosphere packaging system containing blueberry and moisture absorbent, J. Food Process. Preserv. 25 (2001) 49.

[26] H.S. Anderson, Controlled atmosphere package, US Patent 4,842,875 (27 June 1989), assigned to Hercules Inc.

[27] M.K. Antoon, Curable silicone-coated microporous films for controlled atmosphere packaging, US Patent 5,160,768 (3 November 1992), assigned to Hercules Inc.

[28] D.R. Paul, Y.P. Yampol'skii (Eds.), Polymeric Gas Separation Membranes, CRC Press, Boca Raton, 1994.

[29] W.S.W. Ho, K.K. Sirkar (Eds.), Membrane Handbook, Nostrand Reinhold (Van), New York, 1992.

[30] R.B. Bird, W.E. Stewart, E.N. Lightfoot, Transport Phenomena, Wiley, New York, 1960.